Molecular BioSystems

RSC Publishing

PAPER

View Article Online
View Journal | View Issue

Cite this: *Mol. BioSyst.*, 2013, **9**, 508

Switching *p*53 states by calcium: dynamics and interaction of stress systems

Md. Jahoor Alam,[a] Gurumayum Reenaroy Devi,[a] Ravins,[a] Romana Ishrat,[a] Subhash M. Agarwal[b] and R. K. Brojen Singh*[a]

Received 13th July 2012,
Accepted 8th January 2013

DOI: 10.1039/c3mb25277a

www.rsc.org/molecularbiosystems

The integration of calcium and a *p*53–*Mdm*2 oscillator model is studied using a deterministic as well as a stochastic approach, to investigate the impact of a calcium wave on single cell dynamics and on the inter-oscillator interaction. The high dose of calcium in the system activates the nitric oxide synthase, synthesizing nitric oxide which then downregulates *Mdm*2 and influences drastically the *p*53–*Mdm*2 network regulation, lifting the system from a normal to a stressed state. The increase in calcium level switches the system to different states, as identified by the different behaviours of the *p*53 temporal dynamics, *i.e.* oscillation death to sustain the oscillation state *via* a mixed state of dampened and oscillation death states. Further increase of the calcium dose in the system switches the system from sustained to oscillation death state again, while an excess of calcium shifts the cell to an apoptotic state. Another important property of the calcium ion is its ability to behave as a synchronizing agent among the interacting systems. The time evolution of the *p*53 dynamics of the two diffusively coupled systems at stress condition *via* Ca^{2+} shows synchronization between the two systems. The noise contained in the system interestingly helps the system to maintain its stabilized state (normal condition). However, noise has the tendency to destruct the synchronization effect, which means that it tries to restrict the system from external signals to maintain its normal condition. However, at the stress condition, the synchronization rate is found to be faster.

Introduction

Cell stress is broadly defined to include cellular responses to heat shock, oxidative stress, heavy metals and toxic chemicals.[1] Cellular stress can lead to the activation of survival pathways or the initiation of cell death. It is also the precursor of many cellular pathways.[2] Cellular stress can be protective or destructive, depending upon the nature and duration of the stress applied, as well as the cell type.[3,4] Cellular death pathways, such as apoptosis, necrosis, pyroptosis, or autophagic cell death, are dependent on various external factors, which shift the normal state to cellular stress.[4] Ca^{2+} is an important signaling agent that plays a role in the transition between cell survival and cell death.[1,2] Ionic calcium induces the synthesis of various vasoactive substances in the endothelium, including nitric oxide, prostacyclin and other prostanoids.[3] It then induces nitric oxide synthases in the cell cytosol, which leads to the production of activated nitric oxide synthases (NOS).[5–7] Activated nitric oxide synthases interact with the arginine present in the cytosol.[8] This interaction allows the production of nitric oxide and citrulline as a by-product.[9] Nitric oxide (NO) is an important messenger molecule that is involved in regulating many cellular functions, including tumour development, metastasis and apoptosis.[10–12] It is an extremely short lived bioactive molecule. Nitric oxide is also an inducer of stress signaling in cells due to its ability to damage proteins and DNA.[13–16] Nitric oxide triggers the apoptosis process, which is associated with *p*53 gene activation.[17,18] Nitric oxide activates *p*53 by down regulating the *Mdm*2 protein.[12] Recent metabolic experimental studies suggest that there are three isoforms of nitric oxide synthases, namely, endothelial (eNOS), neuronal (nNOS) and inducible (iNOS) forms.[7,9] All three types of nitric oxide synthases are activated through different extra and intra stimuli. It has been also reported that NO produced by nNOS and eNOS has a signalling role and are under the strict control of intracellular calcium ions.[4,19]

*p*53 is one of the most frequently mutated genes in human cancers and, as a result, is one of the most well studied genes in the history of cancer research.[20,21] *p*53 is involved in many key regulations, such as the prevention of cancer formation, including cell cycle arrest, DNA repair and apoptosis.[22,23] *p*53 is

[a] *Center for Interdisciplinary Research in Basic Science, Jamia Millia Islamia, New Delhi, 110025, India. E-mail: rksingh@jmi.ac.in; Fax: +91 2698 1717 (4492); Tel: +91 2698 3409 (4492)*

[b] *Bioinformatics Division, Institute of Cytology and Preventive Oncology, 1-7, Sector - 39, Noida 201301, India*

a tumour suppressor protein that acts as a major hub for many complex signaling pathways that have evolved to sense a broad range of cellular stresses, including DNA damage, oncogene activation, nucleotide depletion, nitric oxide and hypoxia.[24] In response to various types of stress, *p*53 becomes activated and this is reflected in elevated protein levels as well as augmented biochemical functions. In normal cells (*i.e.* under unstressed conditions), *p*53 is a short-lived protein whose activity is maintained at a low level[25] through its interaction with the *Mdm*2 protein, which targets *p*53 for proteasomal degradation. *p*53 acts as a transcription factor which transcriptionally activates the *Mdm*2 gene to form *Mdm*2–mRNA, due to which production of the *Mdm*2 protein increases in the cells.[26–35] *Mdm*2 acts as a negative feedback regulator for *p*53.[19,36,37] After forming the complex, *Mdm*2 ubiquitinates *p*53 due to which the level of *p*53 decreases,[20,25,38–48] and this leads to the oscillatory behaviour of *p*53 inside the cell.

However, even though several models have been developed so far for capturing the oscillatory dynamics of the *p*53–*Mdm*2 network pathway, how ionic calcium activates the *p*53–*Mdm*2 network is not yet studied. The different roles of Ca^{2+} in providing various state conditions and in correlating stress cells are still open questions. The role of noise in cellular organization is also important, and needs to be investigated systematically. In this present work, we raise these questions in Ca^{2+} induced stress cells *via* a *p*53–*Mdm*2 network and through the intercellular interaction of such coupled systems *via* Ca^{2+}. We aim to study an integrated model consisting of two different oscillators, namely calcium and *p*53–*Mdm*2 oscillators, and investigate the influence of ionic calcium to identify the dynamical behaviour of the variables, both in individual cells and a group of cells.

Materials and methods

The biochemical reaction network of the two-oscillator system which consists of Ca^{2+} and *p*53–*Mdm*2 oscillators is presented. The interaction between these two oscillators, *via* the small but short lived molecule NO, and activated by the Ca^{2+} concentration level in the system, is studied to understand the dynamics of *p*53. Further, the synchronization among the diffusively coupled identical two-oscillator systems (one dimensional array) *via* a coupling agent Ca^{2+} is studied. We explain the methods employed to study the system in the following sections.

Calcium oscillator model

The basic single cell model of the calcium oscillation proposed by Houart *et al.*[49] and Jahoor *et al.*[50] involves the feedback regulation of cytosolic and internally stored Ca^{2+} *via* the self-regulator IP_3 signal (Fig. 1). The biochemical reaction network of the model comprises of three key regulators, namely, the free cytosolic calcium (x_7), the internally stored Ca^{2+} in the internal pool (x_8) and the IP_3 molecule (x_9), see Table 1 for reference. Further, the net flux of calcium in and out of the cell (X_6) is also being considered to indicate the overall calcium level[51] in the cell: $X^* = X_6 + X_7$. If we define a population state vector $\vec{Y}'(t) = [X_6,\ldots,X_9]^T$, at any instant of time t, then the time evolution of the state vector is given by the following chemical Langevin equation,[52]

$$\frac{\mathrm{d}\vec{Y}(t)}{\mathrm{d}t} = \vec{F}(x_6,\ldots,x_9) + \frac{1}{\sqrt{V}}\vec{F}_L(x_6,\ldots,x_9;\,\xi_i) \qquad (1)$$

where, $\vec{Y}(t) = \frac{1}{V}\vec{Y}'(x) = [x_6,\ldots,x_9]^T$ is the concentration vector with V as the system size. The second term is the noise term derived from the stochastic description of the interacting molecular system, by allowing two realistic approximations; firstly, when $\Delta t \to 0$, where Δt in $[t,t+\Delta t]$ is the time the reaction was started, the propensity function remains fixed, and secondly, when $\Delta t \to \infty$, this leads to a large propensity function, which is true for a natural system. $\{\xi_i\}$ is the set of Wannier or random parameters. The eqn (1) becomes deterministic at the thermodynamic limit defined by $V \to \infty$ and $N \to \infty$, but $N/V \to$ finite. N is the number of molecules in the system, and is given by: $\frac{\mathrm{d}\vec{Y}(t)}{\mathrm{d}t} = \vec{F}(x_6,\ldots,x_9)$. The functional vectors $\vec{F}$ and $\vec{F}_L$ are given by,

$$\vec{F}(x_6,\ldots,x_9) = \begin{pmatrix} k_9 \\ V_0 + V_1\beta - V_2 + V_3 + k_f x_8 - k x_7 \\ V_2 - V_3 - k_f x_8 \\ \beta V_4 - V_5 - k_{10} x_9 \end{pmatrix}$$

$$\vec{F}_L(x_6,\ldots,x_9;\,\xi_i) = \begin{pmatrix} \sqrt{k_9}\xi_1 \\ \left[\sqrt{V_0}\xi_2 + \sqrt{V_1\beta}\xi_3 - \sqrt{V_2}\xi_4 + \sqrt{V_3}\xi_5 + \sqrt{k_f x_8}\xi_6 \right. \\ \left. -\sqrt{k x_7}\xi_7\right] \\ \sqrt{V_2}\xi_8 - \sqrt{V_3}\xi_9 - \sqrt{k_f x_8}\xi_{10} \\ \sqrt{\beta V_4}\xi_{11} - \sqrt{V_5}\xi_{12} - \sqrt{k_{10} x_9}\xi_{13} \end{pmatrix}$$

where the values or expressions for V_0, V_1, V_2, V_3, V_4 and V_5 are given in Table 2. V_0 indicates the constant input of Ca^{2+}, and V_1 returns to a maximum rate of stimulus induced influx of Ca^{2+} from the extracellular medium. The parameter β is the degree of stimulation of the cell, and V_1 and V_2 are the pumping and release of Ca^{2+} from cytosol to the internal store and the internal store to cytosol, respectively, in the Ca^{2+}-induced Ca^{2+} release process with the maximum rates V_{M2} and V_{M3}. C_2, C_x, C_y and C_z are the threshold values of the release, pumping and activation of release by Ca^{2+} and IP_3 respectively. k_{16} is the passive, linear leak rate constant; k_{10} is the rate of Ca^{2+} diffusing into extracellular medium; V_4 relates to the rate of stimulus-induced synthesis of x_9 and V_5 is the phosphorylation rate of x_9 by the 3-kinase.

The Hill equation of the forms V_2, V_3 and V_5 is given in Table 2 (expressions in the chemical reaction channel numbers 12, 13 and 17), and is obtained from the feedback type of pumping and release of Ca^{2+} from cytosol to the internal store and then the internal store to cytosol in a co-operative manner, and the rate of phosphorylation of IP_3 at equilibrium.

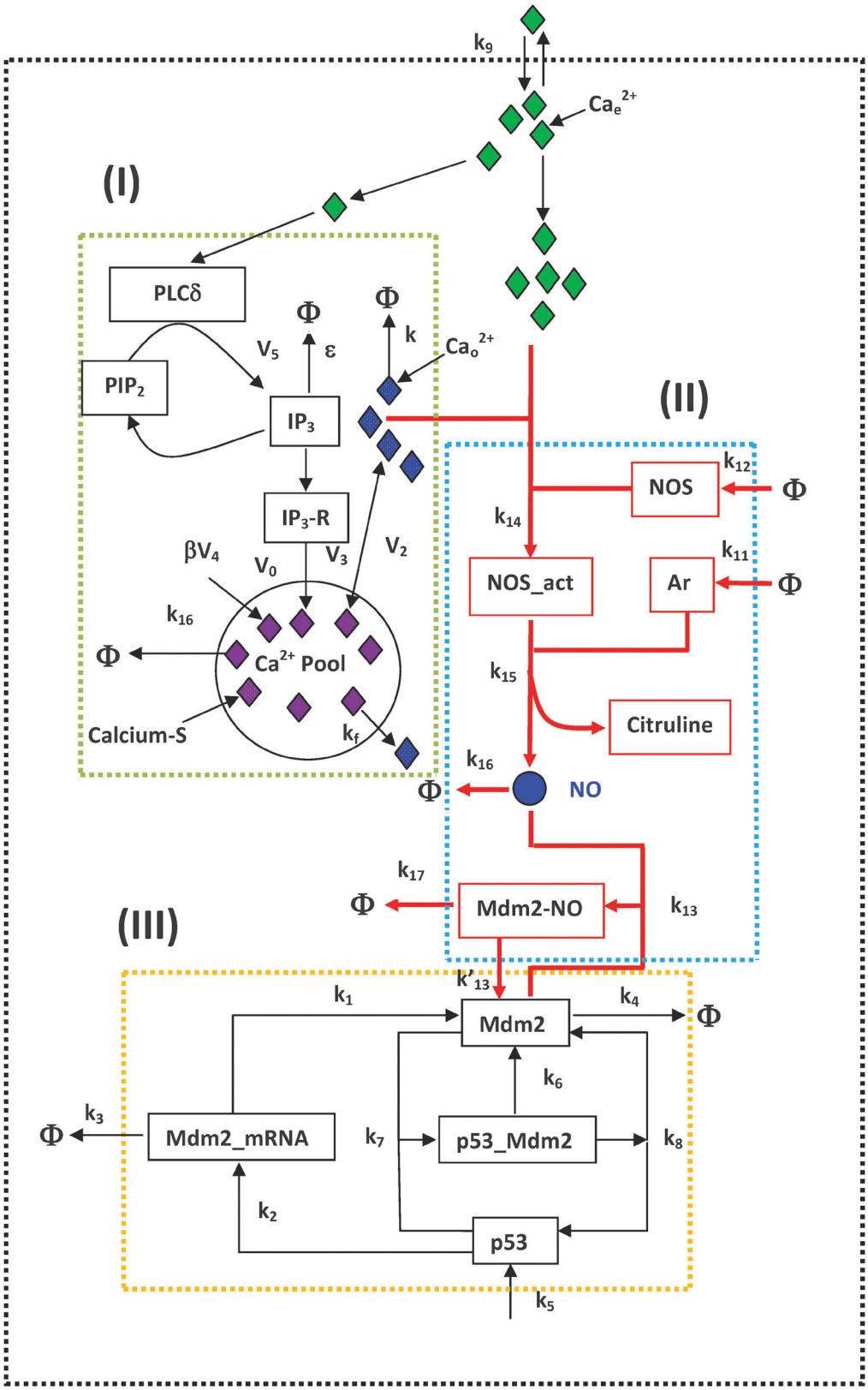

Fig. 1 Schematic model of the reaction network.

These are already assumed to be included in the corresponding single reactions, respectively, *via* these equations.[53] It is used to estimate how many target molecules can bind to a receptor[53] to produce a significant functional effect.[54] The Hill coefficient

Table 1 List of molecular species

Sl. No.	Molecular Species	Description	Notation
1	*p*53	Unbound *p*53 protein	X_1
2	*Mdm*2	Unbound *Mdm*2 protein	X_2
3	*p*53–*Mdm*2	*p*53–*Mdm*2 protein	X_3
4	*Mdm*2–mRNA	*Mdm*2 messenger RNA	X_4
5	NO–*Mdm*2	*Mdm*2–NO complex	X_5
6	Ca_e^{2+}	Extracellular calcium	X_6
7	Ca_o^{2+}	Released calcium from internally stored calcium	X_7
8	Calcium-S	Stored calcium in pool	X_8
9	IP_3	Unbound *p*53 protein	X_9
10	NOS	Nitric oxide synthase	X_{10}
11	NO	Unbound nitric oxide	X_{11}
12	Ar	Unbound arginine	X_{12}
13	NOS–*act*	Activated nitric oxide synthase	X_{13}

Table 2 List of chemical reactions, their kinetic laws and their rate constant

Sl. No.	Reaction channel	Description	Kinetic laws	Values of rate constant	References
1	$X_4 \xrightarrow{k_1} X_4 + X_2$	*Mdm*2 translation	k_1X_4	4.95×10^{-4} s^{-4}	22,32
2	$X_1 \xrightarrow{k_2} X_1 + X_4$	Synthesis of *Mdm*2–mRNA	k_2X_1	1.0×10^{-4} s^{-1}	22,32
3	$X_4 \xrightarrow{k_3} \phi$	Degradation of *Mdm*2–mRNA	k_3X_4	1.0×10^{-4} s^{-1}	22,32
4	$X_2 \xrightarrow{k_4} \phi$	Degradation of *Mdm*2	k_4X_2	4.33×10^{-4} $s^{-}1$	22,32
5	$\phi \xrightarrow{k_5} X_1$	Synthesis of *p*53	k_5	0.78 s^{-1}	22,32
6	$X_3 \xrightarrow{k_6} X_2$	Decay of *p*53	k_6X_3	8.25×10^{-4} s^{-1}	22,32
7	$X_1 + X_2 \xrightarrow{k_7} X_3$	Synthesis of *p*53–*Mdm*2 complex	$k_7X_1X_2$	11.55×10^{-4} mol^{-1} s^{-1}	22,32
8	$X_3 \xrightarrow{k_8} X_1 + X_2$	Degradation of *p*53–*Mdm*2 complex	k_8X_3	11.55×10^{-6} s^{-1}	22,32
9	$\phi \xrightarrow{k_9} X_6$	Diffusion of Ca_e^{2+} from extra-cellular medium to the cell	k_9	1×10^{-2} mol^{-1} s^{-1}	49
10	$\phi \xrightarrow{V_0} X_7$	Constant input of Ca_o^{2+} inside the cell	V_0	2.0 s^{-1}	47,48
11	$\phi \xrightarrow{\beta V_1} X_7$	Stimulus-induced influx of calcium from extracellular medium	βV_1	$\beta = 0.5$, $V_1 = 2.0$	47,48
12	$X_7 \xrightarrow{V_2} X_8$	Pumping of Ca_o^{2+} from cytosol to the internal calcium pool	$V_2 = V_{M2}\frac{X_7^2}{C_2^2 + X_7^2}$	$V_{M2} = 6$, $C_2 = 0.1$	47,48
13	$X_8 \xrightarrow{V_3} X_7$	Release of Ca_o^{2+} from the calcium pool to cytosol	$V_3 = V_{M3}\frac{X_7^m}{C_x^m + X_7^m}\frac{X_8^2}{C_y^2 + X_8^2}\frac{X_9^4}{C_z^4 + X_9^4}$	$V_{M3} = 20$, $m = 2$, $C_x = 0.5$, $C_y = 0.2$, $C_z = 0.2$	47,48
14	$X_8 \xrightarrow{k_f} X_7$	Release of Ca_o^{2+} from the calcium pool to Cytosol due to leakage	k_fX_8	0.01	47,48
15	$X_7 \xrightarrow{k} \phi$	Decay of Ca_o^{2+}	kX_7	1.0	47,48
16	$\phi \xrightarrow{\beta V_4} X_9$	Stimulus-induced synthesis of IP_3	βV_4	$\beta = 0.5$, $V_4 = 2.0$	47,48
17	$X_9 \xrightarrow{V_5} \phi$	Phosporylation of IP_3 by 3-kinase	$V_5 = V_{M5}\frac{X_9^p}{C_s^p + X_9^p}\frac{X_7^n}{C_d^n + X_7^n}$	$V_{M5} = 5.0$, $p = 2.0$, $C_5 = 1.0$, $n = 4.0$, $C_d = 0.4$	47,48
18	$X_9 \xrightarrow{k_{10}} \phi$	Decay of IP_3	$k_{10}X_9$	0.01 s^{-1}	47,48
19	$\phi \xrightarrow{k_{11}} X_{12}$	Synthesis of arginine	k_{11}	0.01 s^{-1}	12
20	$\phi \xrightarrow{k_{12}} X_{10}$	(NOS)	k_{12}	0.0001 s^{-1}	12
21	$X_{11} + X_2 \xrightarrow{k_{13}} X_5$	Synthesis of *Mdm*2–NO complex	$k_{13}X_{11}X_2$	1.0×10^{-3} s^{-1}	12
22	$X_5 \xrightarrow{k'_{13}} X_{11}$	Degradation of *Mdm*2–NO complex	$k'_{13}X_5$	3.3×10^{-4} s^{-1}	12
23	$X^* + X_{10} \xrightarrow{k_{14}} X_{13}$	Formation of NOS–*act*	$k_{14}X^*X_{10}$	10.0 s^{-1}	12
24	$X_{12} + X_{13} \xrightarrow{k_{15}} X_{11} + \text{citruline}$	Synthesis of nitric oxide and citrulline as by-product	$k_{15}X_{12}X_{13}$	10.0 s^{-1}	12
25	$X_{11} \xrightarrow{k_{16}} \phi$	Decay of nitric oxide	$k_{16}X_{11}$	0.001 s^{-1}	12
26	$X_5 \xrightarrow{k_{17}} \phi$	Decay of *Mdm*2–NO	$k_{17}X_5$	0.001 s^{-1}	12

(n, m and p in the Hill equations are positive integers) is generally defined as the interaction coefficient or index of co-operativity, and can be used to accurately estimate the minimum number of binding sites reflected from the co-operativity present.[53–55] The estimation leads to the values of the Hill coefficients in the model studied to be $m = 2$, $n = 4$ and $p = 2$ respectively.

*p*53–*Mdm*2 Oscillator model

*p*53 is a highly integrated and hugely connected protein in a cell that is constantly produced[28] to take part in various biological functions. The interaction of *p*53 and *Mdm*2 maintains a minimum *p*53 level in normal cells. Even though these proteins are available both in the cytoplasm and the nucleus, after activation they localize in the nucleus where they activate target genes.[41,42] The model studied shows how *p*53 transcriptionally activates *Mdm*2, however, *Mdm*2 negatively regulates *p*53,[25,43–45,47] which in turn forms a *Mdm*2–mRNA.[26,48] This *Mdm*2–mRNA leads to the formation of the *Mdm*2 protein and is then exported to the cytoplasm. The *Mdm*2 protein is then exported to the nucleus from the cytoplasm and interacts with *p*53 to form a tight *p*53–*Mdm*2 complex.[29,30,40] This complex formation allows *Mdm*2 to inhibit *p*53 transcriptional activity and also stimulates the degradation of *p*53.[30–32,40] The half life periods of *Mdm*2 and *p*53 are around 30 minutes[33,39] and 15–25 minutes,[33] respectively, which are very short. The half life period of *Mdm*2–mRNA is reported to be 60–120 minutes.[27,35] As a result of the short life time of these proteins and complexes, the rate of creation and decay is extremely short. Thus, this process produces oscillation in *p*53 and *Mdm*2 in the *p*53–*Mdm*2 network *via* a feedback loop. The reaction channels with the transition rates and values of the rate constants of the *p*53–*Mdm*2 network are given in Table 2. If the state of the system at any instant of time t is given by $\vec{Z}(t) = \frac{1}{V}[X_1, ..., X_5]^T = [x_1, ..., x_5]^T$, then the time evolution of the network is given by,

$$\frac{d\vec{Z}(t)}{dt} = \vec{G}(x_1, ..., x_5) + \frac{1}{\sqrt{V}}\vec{G}_L(x_1, ..., x_5; \xi_i) \qquad (2)$$

where, the functional vectors $\vec{G}$ and $\vec{G}_L$ are given by,

$$\vec{G}(x_1, ..., x_5) = \begin{pmatrix} k_5 - k_7 x_1 x_2 + k_8 x_3 \\ k_1 x_4 - k_4 x_2 + k_6 x_3 - k_7 x_1 x_2 + k_8 x_3 - k_{13} x_2 x_{11} \\ -k_6 x_3 + k_7 x_1 x_2 - k_8 x_3 \\ k_2 x_1 - k_3 x_4 \\ k_{13} x_2 x_{11} - k'_{13} x_5 \end{pmatrix}$$

$$\vec{G}_L(x_1, ..., x_5; \xi_i) = \begin{pmatrix} \sqrt{k_5}\xi_{14} - \sqrt{k_7 x_1 x_2}\xi_{15} + \sqrt{k_8 x_3}\xi_{16} \\ \left[\sqrt{k_1 x_4}\xi_{17} - \sqrt{k_4 x_2}\xi_{18} + \sqrt{k_6 x_3}\xi_{19}\right. \\ \left. -\sqrt{k_7 x_1 x_2}\xi_{20} + \sqrt{k_8 x_3}\xi_{21} - \sqrt{k_{13} x_2 x_{11}}\xi_{22}\right] \\ -\sqrt{k_6 x_3}\xi_{23} + \sqrt{k_7 x_1 x_2}\xi_{24} - \sqrt{k_8 x_3}\xi_{25} \\ \sqrt{k_2 x_1}\xi_{26} - \sqrt{k_3 x_4}\xi_{27} \\ \sqrt{k_{13} x_2 x_{11}}\xi_{28} - \sqrt{k'_{13} x_5}\xi'_{28} \end{pmatrix}$$

Nitric oxide is constantly produced in various cells due to enzyme metabolism.[14,15] Ionic calcium acts as a precursor to those enzymes.[4,19] The calcium level in a cell is considered to be obtained from two sources, one from the internal Ca^{2+} pool (from the calcium oscillator given by (I) in Fig. 1), and the other from the extracellular calcium influx by direct diffusion from outside the cell. The overall calcium level interacts with the nitric oxide synthase (x_{10}) and the nitric oxide synthase gets activated (x_{13}). The activated nitric oxide synthase interacts with arginine (x_{12}) to produce nitric oxide and citrulline as a by-product.[5–9] The level of nitric oxide formed in the cell depends on the level of calcium, and can interact with the *p*53–*Mdm*2 oscillator *via* the *Mdm*2 protein, forming the NO–*Mdm*2 complex (x_5) (Fig. 1).[12,56] Even if the half life period of the nitric oxide is very short, only around 5–10 seconds,[12,15] it can move a distance of a few hundreds of cells from the site of its synthesis. Hence, the nitric oxide molecule is believed to be one of the most important intracellular and intercellular signaling molecules. In this model, the extracellular influx of the nitric oxide molecule is not considered by assuming that the amount of nitric oxide created in the cell *via* calcium is much more, as compared to the extracellular influx nitric oxide. Since nitric oxide downregulates *Mdm*2, it eventually affects the dynamics of the *p*53 that leads to the fluctuation of the *p*53 level and stabilization.[12,40,56,57] The nitric oxide molecule is considered to be a unidirectional signaling molecule (from the calcium oscillator to the *p*53–*Mdm*2 oscillator) to study the impact of the calcium ion on *p*53 dynamics and regulation. If we consider $\vec{S}(t) = \frac{1}{V}[X_{10}, ...X_{13}]^T = [x_{10}, ..., x_{13}]^T$ as the state of the system that connects the two oscillators (calcium and *p*53–*Mdm*2 oscillators) unidirectionally at any instant of time t, the dynamics of the system is given by,

$$\frac{d\vec{S}(t)}{dt} = \vec{H}(x_{10}, ..., x_{13}) + \frac{1}{\sqrt{V}}\vec{H}_L(x_{10}, ..., x_{13}; \xi_i) \qquad (3)$$

where, the functional vectors $\vec{H}$ and $\vec{H}_L$ are given by,

$$\vec{H}(x_{10}, ..., x_{13}) = \begin{pmatrix} k_{12} - k_{14} x^* x_{10} \\ -k_{13} x_2 x_{11} + k'_{13} x_5 + k_{15} x_{12} x_{13} - k_{16} x_{11} \\ k_{11} - k_{15} x_{12} x_{13} \\ k_{14} x^* x_{10} - k_{15} x_{12} x_{13} \end{pmatrix}$$

$$\vec{H}_L(x_{10}, ..., x_{13};\ \xi_i) = \begin{pmatrix} \sqrt{k_{12}} - \sqrt{k_{14} x^* x_{10}}\xi_{29} \\ \left[-\sqrt{k_{13} x_2 x_{11}}\xi_{30} + \sqrt{k'_{13} x_5}\xi'_{30} + \sqrt{k_{15} x_{12} x_{13}}\xi_{31}\right. \\ \left. -\sqrt{k_{16} x_{11}}\xi_{32}\right] \\ \sqrt{k_{11}} - \sqrt{k_{15} x_{12} x_{13}}\xi_{33} \\ \sqrt{k_{14} x^*}\xi_{34} - \sqrt{k_{15} x_{12} x_{13}}\xi_{35} \end{pmatrix}$$

The calcium and *p*53–*Mdm*2 oscillators defined by eqn (1) and (2) are now unidirectionally (from the calcium to *p*53–*Mdm*2 oscillator)

connected *via* a nitric oxide pathway given by eqn (3). The dynamics of the two oscillators can be studied by solving the coupled eqn (1)–(3), using the standard 4th order Runge–Kutta algorithm.[58]

Signal processing between the two systems can be studied by investigating how the two systems communicate and become synchronized.[59–62] The synchronization between the two signals defined by the ith variables, $x_i^{[1]}(t)$ and $x_i^{[2]}(t)$ in the two systems can be detected quantitatively by measuring the distance function parameter, $D_{x_i^{[1]},x_i^{[2]}}(t) = ||x_i^{[1]}(t) - x_i^{[2]}(t)||$.[59,63,64] The two systems are in (i) a synchronous state if $D_{x_i^{[1]},x_i^{[2]}}(t) \to 0$, (ii) an uncoupled state if $D_{x_i^{[1]},x_i^{[2]}}(t)$ fluctuates randomly, and (iii) a transition state if the rate of fluctuation about a constant value is $0\left\langle D_{x_i^{[1]},x_i^{[2]}}(t)\right\rangle$ fluctuation (in uncoupled case). Another way of measuring the rate of the synchronization qualitatively is to measure the rate of convergence of the points towards the diagonal in a two dimensional recurrence plot of the corresponding variables of the two systems.[59] The two systems are desynchronized if the points in the plot are scattered randomly away from the diagonal, however, the two systems are strongly synchronized if the points concentrate towards the diagonal.[59]

Results and discussion

The impact of calcium ions on the *p*53–*Mdm*2 network *via* nitric oxide, in a single two-oscillator system, is first investigated numerically by solving eqn (1)–(3). The simulation results both for the deterministic and stochastic systems are presented and compared. The role of noise in the system is discussed in the context of the model we studied. The obtained results are compared with various experimental results reported so far and are found to be in agreement. Further, the synchronization *via* the Ca^{2+} ion between the two diffusively coupled identical systems is then studied to understand the signal processing between them.

Single cell results: impact of Ca^{2+} on *p*53

We first present the deterministic results of the single two-oscillator system showing the impact of Ca^{2+} on *p*53 dynamics in Fig. 2. The level of Ca^{2+} is determined by the combined effect of Ca^{2+} from the calcium oscillator and extracellular Ca^{2+} influx.[51] The rate constant k_{ca} is defined as the overall rate of calcium production in the system, which is equivalent to the combined rate of calcium transported from the internal pool to the cytoplasm (k_{11}, a constant) and rate of extracellular calcium influx (k_{10}, a variable). The low level of Ca^{2+} ($k_{ca} = 0.00005$) does not affect the normal behaviour of *p*53 and *Mdm*2 dynamics too much (Fig. 2), showing dampened oscillations for a few hours (within the interval 0–20 h) and then exhibiting oscillation death, indicating the steady states of *p*53 and *Mdm*2 dynamics. As the value of k_{ca} increases ($0.00005 < k_{ca} < 0.0005$), the activation time ($T_s$), (defined as the time during which *p*53 or *Mdm*2 dynamics show dampened oscillations (regime of activation) and above, where its dynamics go to oscillation death (regime of stabilization)), starts increasing with the amplitude, showing an increase in Ca^{2+} level, which then activates the *p*53 or *Mdm*2 dynamics (Fig. 2). With a further increase in k_{ca} ($0.0005 \le k_{ca} < 0.008$), $T_s \to \infty$ switches to sustain the oscillation regime (regime of complete activation) of these variables *via* the calcium ions. This sustained oscillation persists even for large values of k_{ca} with increasing amplitude as k_{ca} increases. However, a further increase in k_{ca} again gives two regimes, an activated regime (dampened oscillation) and a stabilized regime (oscillation death) but at higher levels of the proteins (Fig. 2). If k_{ca} is increased further, T_s becomes shorter, and at $k_{ca} \ge 0.03$ stabilization of the proteins dominates. This reveals the possible indication of apoptosis because of the excess calcium level, which leads to the synthesis of excess levels of NO.[9,65–67] Depending upon the value of k_{ca} we identify three distinct regimes; (a) the stabilization regime (*p*53 or *Mdm*2 shows oscillation death behavior): for small k_{ca} normal behavior is maintained, but for $k_{ca} \ge 0.03$ cell goes to apoptosis, (b) part activation and part stabilization (dampened oscillation and oscillation death of the proteins): *p*53 and *Mdm*2 are initially activated first for some time and then stabilized, and (c) complete activation (sustained oscillation): the proteins are activated completely depending on a certain calcium level. This claim is supported by two dimensional plots in Fig. 2, the lower panels indicate the three regimes as oscillation death (stabilization), sustained oscillation (activation) and dampened oscillation (part activation and part stabilization).

Further, the period of oscillation of *Mdm*2 in the sustained oscillation regime, obtained by simulating the model we studied after inducing stress *via* a calcium influx, is found to be 4.5 ± 0.58 h, which is in agreement approximately with the reported experimental observation (time period of oscillation is 4–7 h with a mean of 5.5 h)[36] with an error of agreement of around 7–18%. The time period of oscillation of the *p*53 dynamics in this model is almost the same as *Mdm*2, and this period remains almost the same in this sustained oscillation regime ($k_{ca} = [0.0005–0.008]$). However, at small ($k_{ca} < 0.0005$) and large ($k_{ca} > 0.008$) values of k_{ca} corresponding to the dampened oscillation regimes, the period of oscillation varies (4.3–6.4 h), which is again closely in agreement with the experimental results of Geva-Zatorsky *et al.*[36]

The role of noise on activation and stabilization of *p*53

To understand the role of internal noise associated with the molecular events, which reflect as fluctuations in the dynamics of each variable in the stochastic system, we solved the chemical Langevin eqn (1)–(3) for a fixed value of k_{ca}, and varied the system size (V) (Fig. 3). The *p*53 dynamics at a small V ($V \le 100$) show mixed behaviors, first activated (dampened oscillation) and then stabilized (oscillation death). The activation time T_s is found to increase as V increases. The *p*53 dynamics become completely activated for $V \ge 1000$. This shows that noise has a destructive tendency towards the activation of the *p*53 dynamics at a low V. The increase in V induces a decrease in the strength of the noise in the dynamics of the *p*53 protein, and as a result *p*53 starts recovering, and sustains oscillation behavior ($T_s \to \infty$), which corresponds to the activation state. Similar results are found in the case of the *Mdm*2 protein also (Fig. 3 right upper panel).

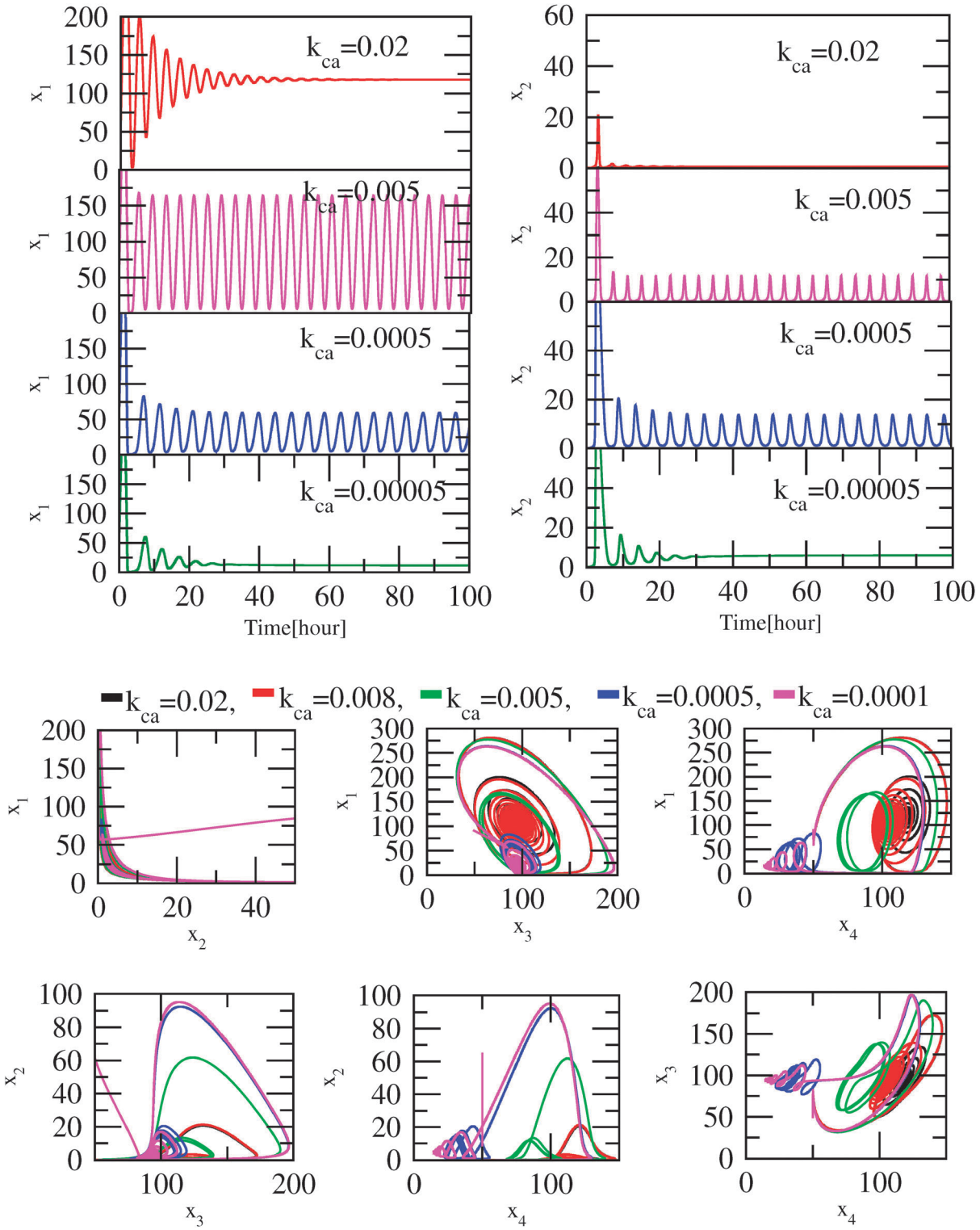

Fig. 2 A plot for the single cell activity with the influence of the calcium ions in a deterministic environment.

The above claim is supported by the two dimensional plots of the various molecular species *i.e.* *p*53, *Mdm*2, *Mdm*2–mRNA and *p*53–*Mdm*2 for the different values of V = 100, 500, 1000 and 5000, respectively (Fig. 3 lower panel). The plots clearly show dampened oscillations (dampened activation) followed by oscillation death (stabilization) for the lower values of V (100). The sustained oscillation of the molecular species, indicated by the broadened limit cycle (complete activation) due to the noise associated with it, is observed for a large V ($\geq$1000).

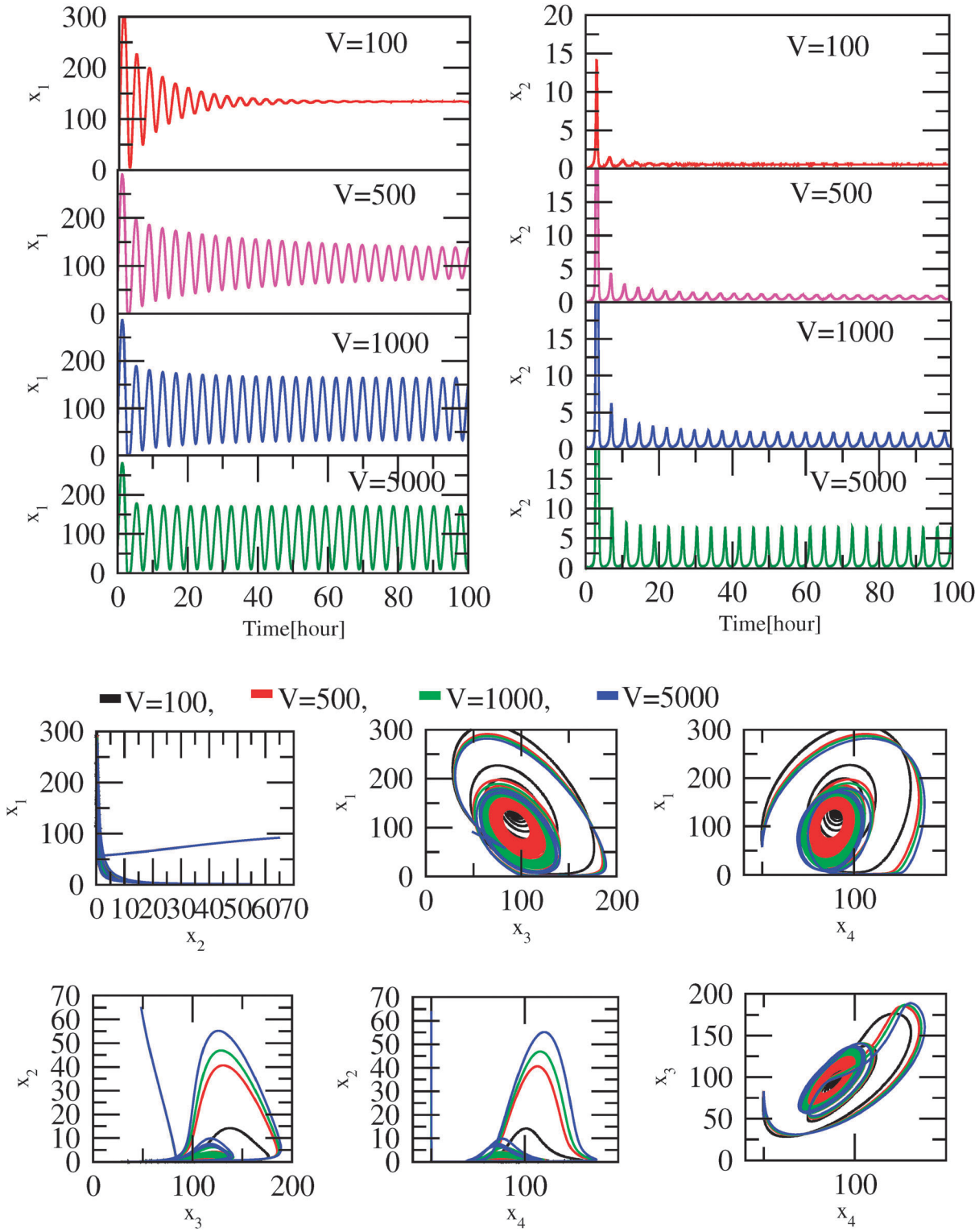

Fig. 3 A plot for the single cell activity with the influence of the calcium ions in a stochastic environment.

Stability analysis in single two-oscillator system

The activation time, T_s, is calculated for the $p53$ dynamics as a function of the calcium level in a single two-oscillator system that can be measured by k_{ca} (Fig. 4). The results are both for the deterministic (Fig. 4 upper panel) and the stochastic (Fig. 4 lower panel) systems, and we found three distinct regimes as shown in the plots. In the deterministic case, for small values of k_{ca} ($0 < k_{ca} < 0.0001$), the T_s value remains almost constant at the lowest value (≈ 23), indicating the stabilized regime leading

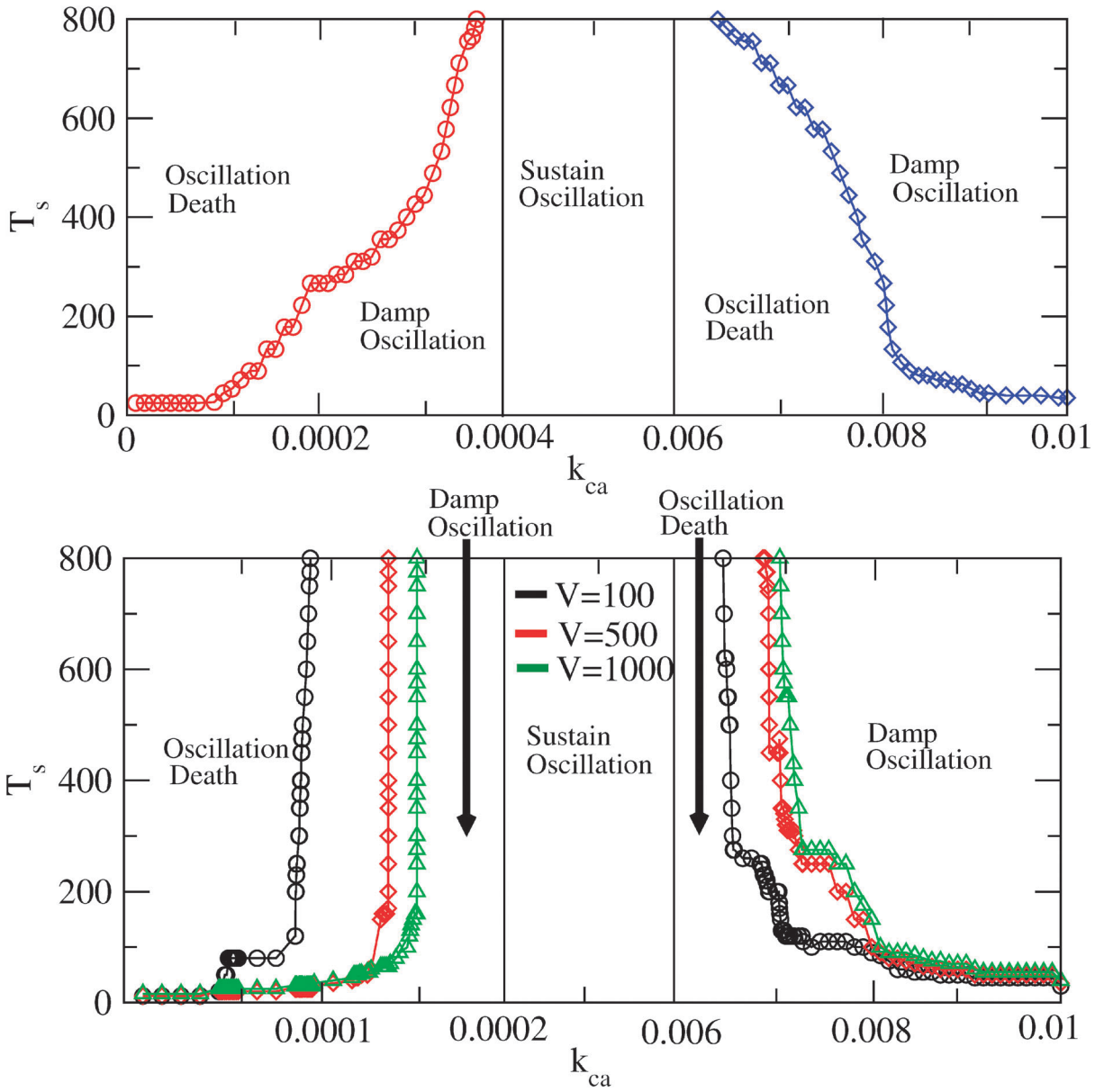

Fig. 4 A plot for the time of stability of the molecule *versus* calcium ion rate constant.

to a normal condition. Then the T_s starts increasing monotonically as a function of k_{ca}, showing a dampened oscillation regime. However, within a particular range of k_{ca} ($0.0004 \leq k_{ca} \leq 0.006$), $T_s \rightarrow \infty$, indicating the sustained oscillation regime. In this regime, the *p*53 protein is considered to be activated to the maximum. However, for $k_{ca} > 0.006$, T_s decreases monotonically as k_{ca} increases, after which ($k_{ca} \geq 0.006$) T_s becomes minimized, indicating an oscillation death regime. The oscillation death regime, which corresponds to the stabilized regime, indicates the possible state leading to cell apoptosis.

In the stochastic system, T_s is calculated by solving the chemical Langevin eqn (1)–(3) as a function of k_{ca} for various values of V (Fig. 4 lower panel). The three distinct regimes are found for three different values of V, similar to the deterministic case. The results show that for smaller values of V, say $V = 100$, all the three regimes are shifted towards smaller values of k_{ca} as compared to the deterministic case: stabilized regime for normal state ($0 \leq k_{ca} \leq 0.00004$), dampened regime (first) ($0.00004 \leq k_{ca} \leq 0.00008$), sustain oscillation regime ($0.00008 \leq k_{ca} \leq 0.006$), dampened oscillation regime ($0.006 \leq k_{ca} \leq 0.008$) and stabilized regime ($0.008 \leq k_{ca} \leq 0.01$). As V increases, the three regimes move towards the regimes found in the deterministic case, which reveals that noise (larger in smaller V) helps the system to reach the three different regimes quickly. The width of the activated regime in all values of V approximately remains the same. Further, the behaviour of the three regimes in the stochastic system tends to recover its deterministic behaviour as $V \rightarrow \infty$, *i.e.* at the thermodynamics limit.

Ca^{2+} signaling: synchronization of interacting identical two-oscillator systems

Ca^{2+} is considered to be an important signaling agent for intercellular signal processing. As explained in the above sections, Ca^{2+} interacts indirectly with *p*53 by activating NOS to synthesize NO to reach *p*53 *via Mdm*2.[12,65] This is considered to be a one way pathway in a single two-oscillator system. To investigate Ca^{2+} signaling in such systems, we took two identical two-oscillator systems and allowed them to interact *via* diffusing Ca^{2+} ions as a coupling agent, with the coupling constant ε. We first present the deterministic results that show the synchronization in the *p*53 dynamics of the two coupled systems (Fig. 5). The value of k_{ca} is set to be 0.005, where the sustained oscillation in *p*53 and *Mdm*2 can be obtained. The reason could be that the phenomenon of synchronization can be well studied and captured in this situation. Coupling in the two systems is switched on at 50 h. It is observed that at a very low value of coupling constant (ε = 0.0001), the two systems behave as uncoupled systems, demonstrated by the independent dynamics of the *p*53 proteins of the two systems (Fig. 5, third row of the upper panel). This claim is made based on the time evolution of $D_{x_1^{[1]},x_1^{[2]}}(t)$, which shows random fluctuations of the points in the plot.[63,64] It is again supported by the random distribution of the points away from the diagonal in

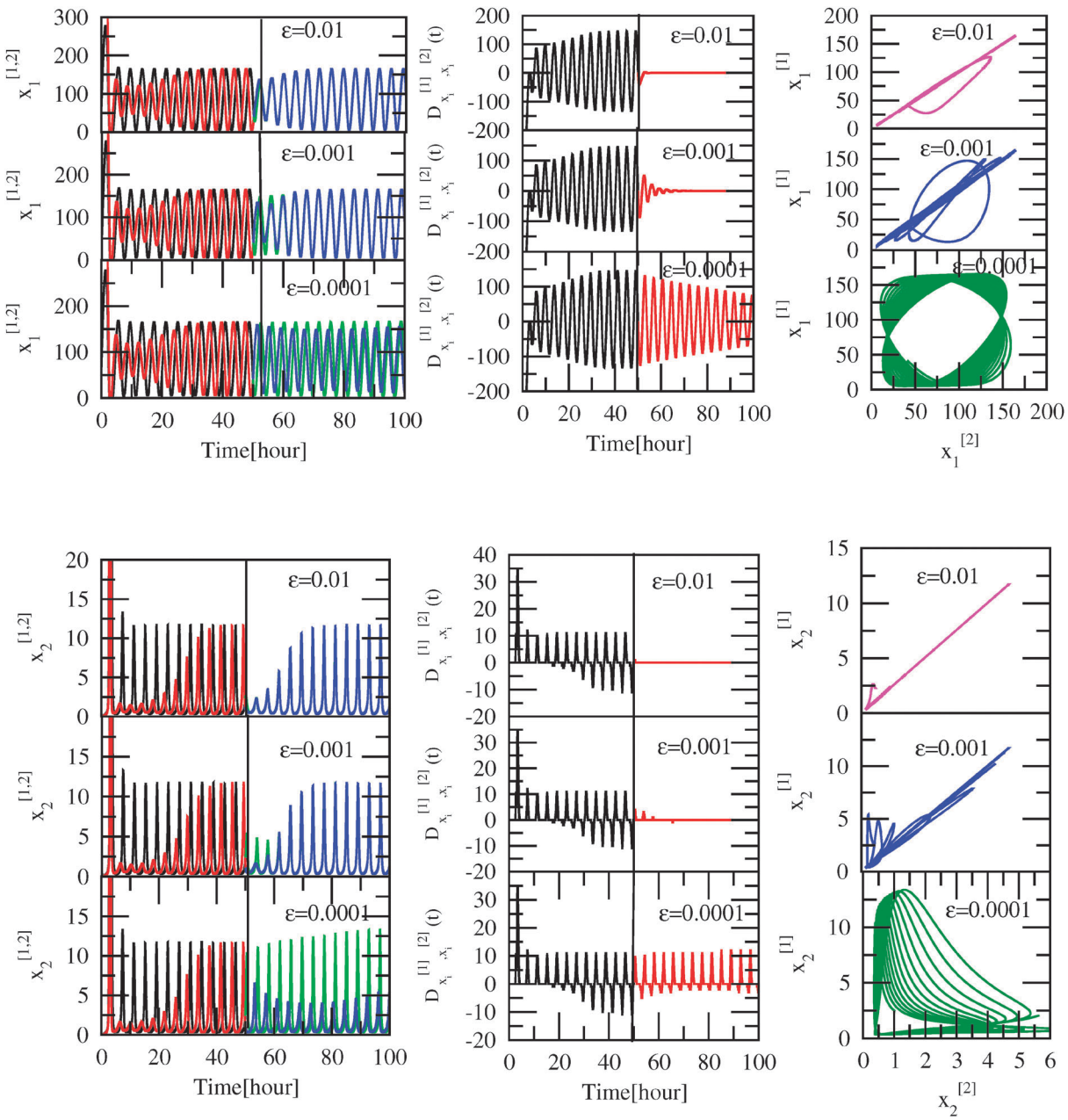

Fig. 5 A plot for the two cell diffusion with the influence of the calcium ions in a deterministic environment.

the two dimensional recurrence plot of $x_1^{[1]}$ and $x_1^{[2]}$ of the two systems.[59] This suggests that at this value of coupling constant, the signal carried by the diffused Ca^{2+} ions is not large enough to process the signal from one system to another, and the systems were not able to communicate with each other. As the value of ε increases (ε = 0.001) the two systems start processing the signal from each other. In this situation, the randomness in the rate of fluctuation of points about a constant value (0) in $D_{x_1^{[1]},x_1^{[2]}}(t)$ *vs* time plot is small, as compared to the fluctuation in the case of ε = 0.0001. Further, the rate of concentration of the points towards the diagonal in the two dimensional recurrence plot in this case is more as compared to the ε = 0.0001 case.

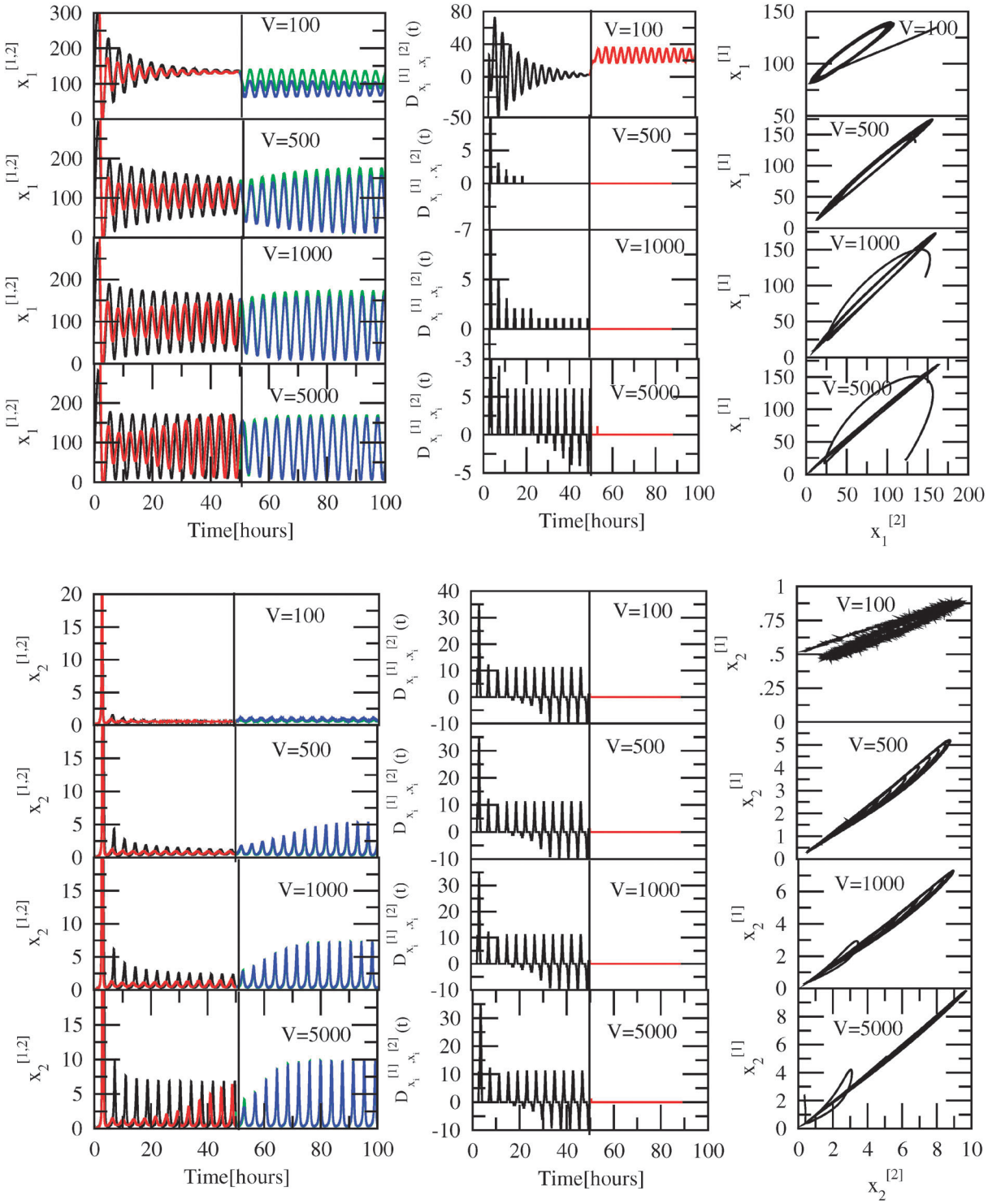

Fig. 6 A plot for the two cell diffusion under influence of noise.

Therefore, the two systems weakly communicate with each other, showing weak synchronization (Fig. 5, second row of upper panel). If the coupling constant is large enough ($\varepsilon = 0.01$), the two systems show strong synchronization indicated by $D_{x_1^{[1]},x_1^{[2]}}(t)$, remaining constant (0) as a function of time. Further, the points in the two dimensional recurrence plots almost lie along the diagonal, supporting the claim of strong synchronization (Fig. 5, first row of upper panel).

The deterministic results of the synchronous dynamics of the *Mdm*2 protein in the two interacting systems with the same parameter values as taken in the case of *p*53, shows similar behaviour of synchronization for all three different values of coupling parameter (Fig. 5 lower panel). The time evolution of $D_{x_1^{[1]},x_1^{[2]}}(t)$ and the two dimensional recurrence plots corresponding to the three values of the coupling constant support this claim. Therefore, the Ca^{2+} wave has an important role in cellular organization and intercellular signal transduction and processing.[50] Since we did not find any significant role of IP_3 in the intracellular *p*53 activation and intercellular synchronization, we do not show the results.

The impact of noise on synchronization

Now we investigate the impact of noise on the synchronization of the coupled systems by simulating the chemical Langevin eqn (1)–(3) of the two coupled stochastic systems. The value of the coupling parameter is taken to be fixed, $\varepsilon = 0.001$ and V is allowed to vary. Coupling is switched on at 50 h. The amount of intrinsic noise contained in a system can be indirectly estimated by varying V: noise associated in the system dynamics increases as V decreases and *vice versa*. The simulation results of the *p*53 dynamics for the two coupled systems at $V = 100$ (Fig. 6, first row of upper panel) show that the *p*53 dynamics of the two systems are evolving independently. The time evolution of $D_{x_1^{[1]},x_1^{[2]}}(t)$ fluctuates randomly, indicating the uncoupled nature of the two systems. It is again supported by the two dimensional recurrence plots, where the points scattered randomly away from the diagonal. However, as V increases ($V \geq 500$) the rate of fluctuations about a constant value (0) decreases, and at $V \geq 1000$ the fluctuation is minimized, showing strong synchronization which is supported by the two dimensional recurrence plots (Fig. 6 upper panel). The results reveal that the noise hinders the phenomenon of synchronization because the uncoupled systems at a high noise level (small V value) become synchronized at a low noise level (high V value).

Similarly, we obtain a similar behaviour in the *Mdm*2 dynamics of the coupled systems as found in the case of *p*53 (Fig. 6 lower panel). Hence noise shows destructive impact on the synchronization of the coupled systems.

Conclusions

The Ca^{2+} ion in the model we studied demonstrates a multifunctional role, for example, it acts both as an activator of *p*53 as well as a synchronizing agent of the coupled systems. The results of our study suggest that the Ca^{2+} level in a cell can activate nitric oxide, which in turn affects the *p*53–*Mdm*2 network by direct interaction with *Mdm*2. The activation of *p*53 by Ca^{2+} in a cell lifts the cell from a normal to a stress state. An excess of Ca^{2+} level leads to the excess production of nitric oxide, shifting the cell to an apoptotic phase, which is also supported by experimental evidence.[6,8] When the cell is in a stress condition, and further if the cell manages to optimize the Ca^{2+} level, the stress state of the cell may revert to its normal state. However, if the cell reaches an apoptotic state, the cell is not able to return to its normal state from the stress state. It indicates that the cell has to manage the Ca^{2+} level to balance its cellular activities and functions.

The important role of Ca^{2+} in intercellular interaction is that it can act as one of the most important synchronizing agents. In general, this phenomenon can be seen in the normal state of the cells. However, this synchronizing activity can also be seen among the interacting stress cells *via* Ca^{2+}, as evident from our investigation. Even though Ca^{2+} reaches *p*53 through two pathway steps *i.e. via* NOS and NO, it still acts as a good synchronizing agent to correlate the activated oscillating *p*53 dynamics in stress cells.

The intrinsic noise due to random molecular interaction in the system can be correlated qualitatively with system size, such that the noise in a small system size is large and *vice versa*.[62] The single cell study reveals that the oscillating (dampened or sustained) temporal dynamics of *p*53 at negligibly small noise (large V) become stabilized (fixed point oscillation) with an increase in noise (small V). This means that the noise associated with the cell helps the cell to maintain its normal condition (stabilized behaviour), trying to prevent stress conditions. Further, noise has a hindrance effect on synchronization. When the cell is at normal conditions (stabilized condition) in a stochastic system, noise prevents it from external signals that may cause stress. Once the system is in a stress condition, external signals are allowed to interfere, which helps to lift the stress and permit the cell to return to its normal condition. However, other important roles of noise need to be investigated both in normal and stress conditions.

Acknowledgements

We thank Prof. R. Ramaswamy and Prof. Pankaj Sharan for their important comments and suggestions in this work. This work is financially supported by the University Grant Commission (UGC), India and carried out at the Center for Interdisciplinary Research in Basic Sciences, Jamia Millia Islamia, New Delhi, India.

References

1 C. Cerella, M. D'alessio, M. D. Nicola, A. Magrini, A. Bergamaschi and L. Ghibelli, *Ann. N. Y. Acad. Sci.*, 2003, **1010**, 74–77.
2 A. Samali, S. Fulda, A. M. Gorman, O. Hori and S. M. Srinivasula, *Int. J. Cell Biol.*, 2010, 2.

3 P. Lopez-Jaramillo, M. C. Gonzalez, R. M. J. Palmer and S. Moncada, *Br. J. Pharmacol.*, 1990, **101**, 489–493.
4 F. Silvagno, H. Xia and D. S. Bredt, *J. Biol. Chem.*, 1996, **271**, 11204–11208.
5 J. T. Hansen, A. Ferreira, S. Yano, D. Kanuparthi, J. R. Romero, E. M. Brown and N. Chattopadhyay, *Am. J. Physiol.: Endocrinol. Metab.*, 2005, **6**, 288.
6 E. N. Dedkova, X. Ji, S. L. Lipsius and L. A. Blatter, *Am. J. Physiol.: Cell Physiol.*, 2004, **286**, C406–C415.
7 R. C. Manser and F. D. Houghton, *J. Cell Sci.*, 2006, **119**, 2048–2055.
8 D. C. Jenkins, I. G. Charles, L. L. Thomsen, D. W. Moss, L. S. Holmes, S. A. Baylis, P. Rhodes, K. Westmore, P. C. Emson and S. Moncada, *Proc. Natl. Acad. Sci. U. S. A.*, 1995, **92**, 4392–4439.
9 R. G. Knowles and S. Moncada, *Biochem. J.*, 1994, **298**, 249–258.
10 J. Zhou and B. Brune, *Toxicology*, 2005, **208**, 223–233.
11 C. V. Rao, *Mutat. Res., Fundam. Mol. Mech. Mutagen.*, 2004, **555**, 107–119.
12 X. Wang, D. Michael, G. D. Muricia and M. Oren, *J. Biol. Chem.*, 2002, **277**, 15697–15702.
13 T. Nguyen, D. Brunson, C. L. Crespi, B. W. Penman, J. S. Wishnok and S. R. Tannenbaum, *Proc. Natl. Acad. Sci. U. S. A.*, 1992, **89**, 3030–3034.
14 J. E. Stern, *Prog. Biophys. Mol. Biol.*, 2004, **84**, 197–215.
15 J. Wood and J. Garthwaite, *Neuropharmacology*, 1994, **33**, 1235–1244.
16 J. Garthwaite and C. L. Boulton, *Annu. Rev. Physiol.*, 1995, **57**, 683–706.
17 C. Q. Li, A. I. Robles, C. L. Hanigan, L. J. Hofseth, L. J. Trudel, C. C. Harris and G. N. Wogan, *Cancer Res.*, 2004, **64**, 3022–3029.
18 H. Okada and T. W. Mak, *Nat. Rev. Cancer*, 2004, **4**, 592–603.
19 J. Wagner, L. Ma, J. J. Rice, W. Hu, A. J. Levine and G. A. Stolovitzky, *IEE Proc.: Syst. Biol.*, 2005, **152**, 109–118.
20 M. Pajkos, B. Meszaros, I. Simon and Z. Dosztanyi, *Mol. BioSyst.*, 2012, **8**, 296–307.
21 X.-F. Liu, H. Zhang, Shi-Guang Zhu, Xian-Ting Zhou, Hai-Long Su, Z. Xu and Shao-Jun Li, *World J. Gastroenterol.*, 2006, **12**(29), 4706–4709.
22 D. P. Lane, *Nature*, 1992, **358**, 15–16.
23 C. J. Proctor and D. A. Gray, *BMC Syst. Biol.*, 2008, **2**, 75.
24 P. Hainaut and K. G. Winman, *25 Years of p53 Research*, Springer, 2007, pp. 141–163.
25 M. H. G. Kubbutat, S. N. Jones and K. H. Vousden, *Nature*, 1997, **387**, 299–303.
26 J. L. Ko, Y. W. Cheng, S. L. Chang, J. M. Su, C. Y. Chen and H. Lee, *Int. J. Cancer*, 2000, **89**, 265–270.
27 S. M. Mendrysa, M. K. McElwee and M. E. Perry, *Gene*, 2001, **264**, 139–146.
28 O. W. Mcbride, D. Merry and D. Givolt, *Proc. Natl. Acad. Sci. U. S. A.*, 1986, **83**, 130–134.
29 A. OBrate and A. Giannakakou, *Drug Resist. Updates*, 2003, **6**, 313–322.
30 U. M. Moll and O. Petrenko, *Mol. Cancer Res.*, 2003, **1**, 1001–1008.
31 R. Honda and H. Yasudaer, *Oncogene*, 2000, **2**, 1473–1476.
32 S. Fang, J. P. Jensen, R. L. Ludwig, K. H. Vousden and A. M. Weissman, *J. Biol. Chem.*, 2000, **2**, 8945–8951.
33 C. A. Finlay, *Mol. Cell. Biol.*, 1993, **13**, 301–306.
34 Y. Pan and D. S. Haines, *Cancer Res.*, 1999, **59**, 2064–2067.
35 A. Hsing, D. V. Faller and C. Vaziri, *J. Biol. Chem.*, 2000, **275**, 26024–26031.
36 N. Geva-Zatorsky, N. Rosenfeld, S. Itzkovitz, R. Milo, A. Sigal, E. Dekel, T. Yarnitzky, Y. Liron, P. Polak, L. Galit and U. Alon, *Mol. Syst. Biol.*, 2006, **2**, 0033.
37 D. Sylvain, N. Henry and P. Jacques, *Trends Genet.*, 2001, **17**, 459–464.
38 N. Tuncbag, G. Kar, A. Gursoy, O. Keskin and R. Nussinov, *Mol. BioSyst.*, 2009, **5**, 1770–1778.
39 Y. Pan and J. Chen, *Mol. Cell. Biol.*, 2003, **23**, 5113–5121.
40 J. Momand, G. P. Zambetti, D. C. Olson, D. George and A. J. Levine, *Cell*, 1992, **2**, 1237–1245.
41 J. Chen, J. Lin and A. J. Levine, *Mol. Med.*, 1995, **1**, 142–152.
42 S. H. Liang and M. F. Clarke, *J. Biol. Chem.*, 1999, **274**, 32699–32703.
43 Y. Barak, T. Juven, R. Haffner and M. Oren, *EMBO J.*, 1993, **12**, 461–468.
44 X. Wu, J. Bayle, H. D. Olson and A. J. Levine, *Genes Dev.*, 1993, **7**, 1126–1132.
45 Y. Haupt, R. Maya, A. Kazaz and M. Oren, *Nature*, 1997, **387**, 296–299.
46 J. Piette, H. Neel and V. Marchal, *Oncogene*, 1997, **15**, 1001–1010.
47 J. Momand, H. H. Wu and G. Dasgupta, *Gene*, 2000, **242**, 15–29.
48 A. Zauberman, D. Flusberg, Y. Haupt, Y. Barak and M. Oren, *Nucleic Acids Res.*, 1995, **23**, 2584–2592.
49 G. Houart, G. Dupont and A. Goldbeter, *Bull. Math. Biol.*, 1999, **61**, 507–530.
50 Md. A. Jahoor, L. Bhayana, G. R. Devi, H. D. Singh, R. K. B. Singh and B. I. Sharma, *J. Chem. Biol.*, 2012, **5**, 27–34.
51 D. J. Adams, J. Barakeh, R. Lanskey and C. V. Breemen, *FASEB J.*, 1989, **3**, 2389–2400.
52 D. T. Gillespie, *J. Chem. Phys.*, 2000, **113**, 297–306.
53 A. V. Hill, *J. Physiol.*, 1910, **40**, iv–vii.
54 J. N. Weiss, *FASEB J.*, 1997, **11**, 835–841.
55 S. Goutelle, M. Maurin, F. Rougier, X. Barbaut, L. Bourguignon, M. Ducher and P. Maire, *Fundam. Clin. Pharmacol.*, 2008, **22**, 633–648.
56 C. M. Schonhoff, M. C. Daou, S. N. Jones, C. A. Schiffer and A. H. Ross, *Biochemistry*, 2002, **41**, 13570–13574.
57 H. Wang, X. Zeng, P. Oliver, L. P. Le, J. Chen, L. Chen, W. Zhou, S. Agrawal and R. Zhang, *Int. J. Oncol.*, 1999, **15**, 653–660.
58 W. H. Press, S. A. Teukolsky, W. T. Vetterling and B. P. Flannery, *Numerical Recipe in Fortran*, Cambridge University Press, 1992.
59 L. M. Pecora and T. L. Caroll, *Phys. Rev. Lett.*, 1990, **64**, 821–824.

60 A. Pikovsky, M. Rosenblum and J. Kurths, *Synchronization: A Universal Concept in Nonlinear Science*, Cambridge University Press, Cambridge, 2001.
61 R. Ramaswamy, R. K. B. Singh, C. Zhou and J. Kurths, *Understanding Complex Systems*, Springer, 2010, pp. 177–193.
62 A. Nandi, G. Santhosh, R. K. B. Singh and R. Ramaswamy, *Phys. Rev. E: Stat., Nonlinear, Soft Matter Phys.*, 2007, **76**, 041136.
63 M. G. Rosenblum and A. S. Pikovsky, *Phys. Rev. Lett.*, 2004, **92**, 114102.
64 M. G. Rosenblum, A. S. Pikovsky and J. Kurths, *Phys. Rev. Lett.*, 1996, **76**, 1804–1807.
65 W. H. Chan, *Int. J. Mol. Sci.*, 2011, **12**, 1041–1059.
66 D. E. Clapham, *Cell*, 2007, 131.
67 T. R. Sodering, B. Chang and D. Brickey, *J. Biol. Chem.*, 2001, 3719–3722.